

TIMING OF ELEVATOR MUSCLE ACTIVITY DURING CLIMBING IN FREE LOCUST FLIGHT

HANNO FISCHER^{1,*} AND WOLFRAM KUTSCH²

¹Zoologisches Institut der Universität zu Köln, Weyertal 119, 50923 Köln, Germany and ²Fakultät für Biologie, Universität Konstanz, 78457 Konstanz, Germany

*e-mail: Hanno.Fischer@uni-koeln.de

Accepted 28 September; published on WWW 29 November 1999

Summary

Despite detailed knowledge of the sensory–motor interactions during elevator muscle timing for the generation of a ‘functional’ flight motor pattern in flying locusts, there is little information about how a possible shift in the onset of elevator activity is correlated with changes in flight variables under closed-loop conditions (i.e. during free flight). Free-flight variables were investigated with respect to ascent angle during climbing flight in locusts *Schistocerca gregaria*. The motor pattern during free flight was examined by telemetric electromyography of particular antagonistic flight muscles in both ipsilateral hemisegments of the pterothorax while flight variables were recorded simultaneously on video. In the majority of

the animals tested, the onset of elevator muscle activity within the wingbeat cycle is delayed when animals increase their ascent angle during climbing flight. In accordance with the motor pattern, the downstroke phase and the stroke amplitude of the wings increased with increasing the ascent angle. This suggests that the relative elevator timing during the wingbeat cycle may be related to the generation of the additional aerodynamic lift required for ascending flight and may, therefore, play a role in the regulation of ascent angle during free flight in the locust.

Key words: locust, free flight, telemetry, motor pattern, flight, behaviour, wingstroke, *Schistocerca gregaria*.

Introduction

The generation of rhythmic motor patterns underlies locomotor behaviour patterns such as walking, swimming and flight. In insects such as locusts, the basic alternating patterns for wing elevation and depression during flight are generated by a neuronal oscillator (e.g. Wilson and Weis-Fogh, 1962; Delcomyn, 1980; Robertson and Pearson, 1985; Stevenson and Kutsch, 1987; Pearson and Wolf, 1987; Wolf and Pearson, 1987) under the influence of afferent information from different sets of proprioceptive sensory organs that can modulate or control the rhythmic output (e.g. Wendler, 1974; Gewecke, 1975; Pearson and Wolf, 1987; Reye and Pearson, 1988; Büschges and Pearson, 1991; Ramirez and Pearson, 1993). This control of the motor pattern is important for flight performance, affecting, for example, lateral stability during flight (Möhl, 1985) and flight steering behaviour (Zarnack and Möhl, 1977; Baker, 1979a,b; Thüning, 1986; Schmidt and Zarnack, 1987).

Sensory input, in general, can influence the timing of both the depressor and elevator muscles during the wingbeat cycle (e.g. Neumann et al., 1983; Möhl, 1985; Horsmann and Wendler, 1985). Furthermore, it has been shown that proprioceptive feedback (in particular from the tegula organs and the wing hinge stretch receptors) plays an important role in timing the onset of elevator activity during flight pattern generation (Wolf and Pearson, 1988; Pearson and Wolf, 1989;

Wolf, 1993). As demonstrated in experiments involving tethered flying locusts or flight preparations, the timing of elevator activity during the wingbeat cycle is of significance during flight not only for the generation of a functional motor pattern (Wolf, 1993) but also during particular flight behaviour patterns (indicated by responses related to roll stimuli or by optomotor reactions associated with flight steering, e.g. Baker, 1979a,b; Thüning, 1986).

Although considerable information is available about motor patterns (including elevator patterning) during steady ‘level’ flight, there is little information about how the locust flight system controls ascending and descending flight paths during free flight. Recently, it was shown that in particular flight muscles the number of motor units recruited during the wingbeat cycle depends on the ascent angle (Kutsch et al., 1999). The first evidence that the timing of elevator activity might play a part in regulating the ascent angle during flight was provided by investigations involving freely flying locusts deprived of afferent information from the tegula (Fischer and Ebert, 1999): although the capability for free flight was maintained even when elevator timing was influenced, the production of the additional effective lifting power required for ascending flight was affected.

To understand more about the functional and behavioural relevance of the modulation of elevator activity during free

locust flight, we focus in the present study on the patterns of antagonistic activity in several depressor and elevator muscles of the fore- and hindwing, on the corresponding wingstroke variables and on the flight behaviour pattern with respect to the ascent angle. The antagonistic motor patterns during free flight were investigated by telemetric electromyography (e.g. Fischer and Ebert, 1999), and the related behavioural patterns were recorded synchronously on video. Wingstroke variables during free flight were documented by high-speed video.

Materials and methods

Animals and flight conditions

All experiments were carried out using adult female *Schistocerca gregaria* Forskål (15–21 days postmoult). The animals were bred at 42 °C and 70% relative humidity under a 12 h:12 h light:dark cycle in crowded colonies of both sexes. Individual flight sequences were investigated in a room measuring 10 m×5.7 m×2.2 m at 34 °C. The average illumination of the room was 4500 lx. All animals were warmed to approximately 40 °C before the flight experiments. To initiate flight, each animal was placed on a platform, and the majority of flights started with the animal jumping (either spontaneously or in response to hand-clapping or a short wind puff to the cerci). When jumping could not be elicited, flight was initiated by launching the animals vertically into the air (speed at release 2–3 m s⁻¹). To avoid any residual effects of the jump and the launch during the observations, the platform and the point of launch were approximately 5 m in front of the observation area. Irrespective of the method of initiating flight (i.e. jump or vertical launching), individual flight sequences ranged from a minimum of 5 s to a maximum of 120 s. Following a launch, the majority of animals performed 4–6 consecutive flight sequences (initiated by spontaneous jump starts from the ground, the walls and the ceiling; the total flight time per animal was, on average, approximately 90 s). Most of the animals crossed the observation area several times when flight activity lasted longer than a few seconds.

Telemetric electromyography

The transmitter device (mass 0.3 g, representing 8–12% of locust body mass) for telemetric acquisition of electromyographic (EMG) data is shown in Fig. 1A. For a description of the circuitry, the attachment of the device to the animal and the receiver system used, see Fischer (1998). One-channel transmission was used to record simultaneously from two ipsilateral muscle antagonists (nomenclature after Snodgrass, 1929). Using three different experimental designs, the forewing muscle activity (1) of the elevator 83 and the subalar depressor 99, (2) of the elevator 90 and 99, and (3) of 83 and the first basalar depressor 97 was investigated. In the hindwing, (1) the elevator 113 and the subalar depressor 129, (2) the elevator 119 and 129, and (3) 113 and the first basalar depressor 127 were examined. Telemetric EMG traces are shown in Fig. 1B. Instantaneous phase values (ϕ) of the specific antagonists were calculated as $\phi_{D/E}=(D-E)/(D-D)$

where $D-E$ is the depressor–elevator interval (in ms) and $D-D$ is the cycle length of the particular depressor (in ms).

Video recordings

The free-flight sequences of individual locusts were recorded using a stationary video camera (Panasonic NV-MS4EG; frame frequency 50 Hz, shuttering time 1 ms). The telemetric EMGs were displayed on an oscilloscope (Tektronix D11) and stored on tape (Racal Store 4DS). The oscilloscope screen was filmed by a second video camera (Revue Video 8, frame frequency 50 Hz, frame interval 20 ms). The video outputs of the two cameras were mixed online (Panasonic digital mixer WJ-AVE5) and recorded on a video master tape.

Wingstroke variables of free-flying locusts (without the transmitter) were determined using a different approach with a digital high-speed video system (maximum frame frequency 500 Hz; shuttering time 500 ms; Weinberger Systems, Switzerland).

The master tape recordings and the high-speed video recordings were both screened on a 27 inch Sony Trinitron colour video monitor and transferred to overhead transparencies for analysis (for methods, see Baker and Cooter, 1979a,b). The free-flight variables (see below) were acquired by frame-by-frame analysis (Panasonic digital video recorder AG7355) of the continuous displacement of the specific body and wing silhouettes. For a detailed evaluation of the measurement error with respect to silhouette length and flight variables, see van der Wall (1996) and Fischer (1998). Motor patterns and wingstroke variables of approximately 15 consecutive wingbeat cycles could be acquired from a flight sequence.

Free-flight variables

The free-flight variables investigated are shown in Fig. 1C. The centre of gravity (at approximately 50% body length; Weis-Fogh, 1956) was chosen as the reference point for the body. The body angle ϕ (degrees) and the ascent angle α (degrees) were measured relative to the horizontal (see also Baker et al., 1981). Stroke amplitudes Ψ (degrees) of the fore- and hindwing were calculated using the cosine equation:

$$\cos\Psi = [(u_w - d_w)^2 - 2L_w^2]/(-2L_w^2), \quad (1)$$

where u_w-d_w is the distance between the upper and lower reversal points of the particular wing (measured from superimposed body silhouettes of consecutive frames) and L_w is the wing length (wing base to wing tip). The duration of wing depression was determined from the time interval between u_w and d_w , and the duration of wing elevation was determined from the time interval between d_w and u_w .

The phase ϕ_{el} of the onset of wing elevation within the wingbeat cycle was determined from:

$$\phi_{el} = (u_w - d_w)/(u_w - u_w). \quad (2)$$

Wingbeat frequency f_{WB} was determined from the time between two consecutive upper reversal points of the wing.

A

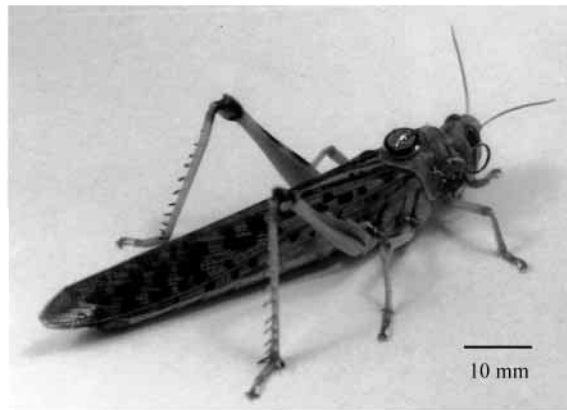
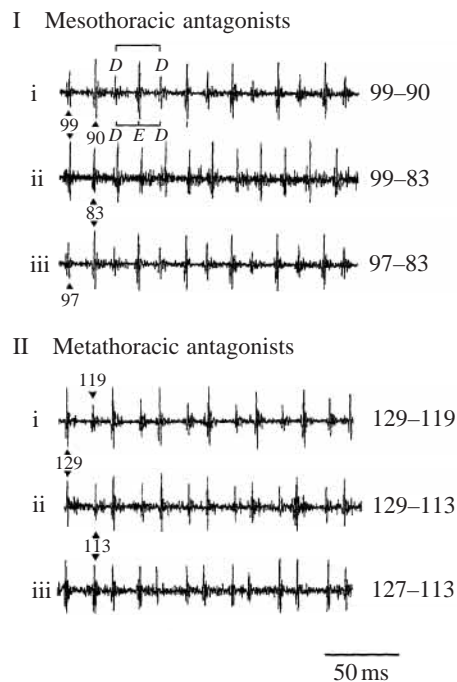
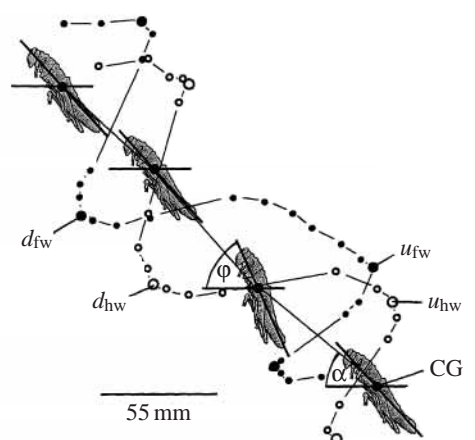


Fig. 1. (A) A mature female desert locust *Schistocerca gregaria* with a transmitter device (mass 0.3 g) attached to its pronotum. Transmitter mass represents on average 8–12% of the body mass. (B) Telemetric electromyographs during locust free flight recorded from the mesothoracic (I) and metathoracic (II) antagonists investigated. *D*, depressor; *E*, elevator. *D–D*, depressor interval; *D–E*, depressor–elevator interval. (C) Flight variables and wingstroke variables evaluated during locust free flight and presented in a schematic drawing reconstructed from high-speed video recordings of freely flying animals (frame interval 2.2 ms). Filled circles reflect the forewing path, and the hindwing path is indicated by open circles. CG, centre of gravity; u_{fw} , u_{hw} , upper reversal point of the fore- and hindwing; d_{fw} , d_{hw} , lower reversal point of fore- and hindwing, respectively; ϕ , angle of the body with respect to the horizontal (degrees); α , angle of ascent with respect to the horizontal (degrees). The distance u_w-d_w (determined by superposition of the body silhouettes) for a particular wing was used to calculate the stroke amplitude Ψ (degrees; for details see text). Flight speed v (m s^{-1}) was deduced from the continuous displacement of the body silhouettes (see also Baker and Cooter, 1979a,b).

B



C



Body length and wing length were measured before the experiments began. All variables were considered as ‘instantaneous’, being constant within the given frame interval.

Statistics

Data analysis and statistical procedures were computer-aided (software KaleidaGraph, StatView and Origin) and follow the criteria described by Sachs (1978). Correlation and linear regression were performed by the method of least square differences at a significance level of $P < 0.05$, with r indicating the coefficient of linear correlation. Two-sample comparisons of the coefficients of regression (i.e. slopes of the regression line) and the intercepts were performed using a t -test (Sachs, 1978) at a significance level of $P < 0.05$. Mean phase values were calculated using circular statistics after the criteria described in Batschelet (1981) and are given as $P \pm$ mean angular deviation, with \mathbf{r} describing the mean vector.

Results

Behavioural variables during climbing free flight

The relationships between body angle ϕ (degrees), ascent angle α (degrees) and flight speed v (m s^{-1}) were determined during free flight at a temperature of 34°C . Eight females (aged 18 days postmoult) were investigated. In addition, to assess how the attachment of a 0.3 g transmitter influenced flight variables, each female performed flights with and without a transmitter: four individuals were equipped with a transmitter after control flights; for the remaining four animals, control variables were recorded after flight performance under loaded conditions. In general, each individual was limited to 20 flight sequences (10 controls and 10 loaded) including those flights in which the animal did not cross the camera focus. The data were evaluated on a per locust basis; for a description of the behaviour of the ‘average’ locust, the data from all animals were pooled. The results are shown in Fig. 2.

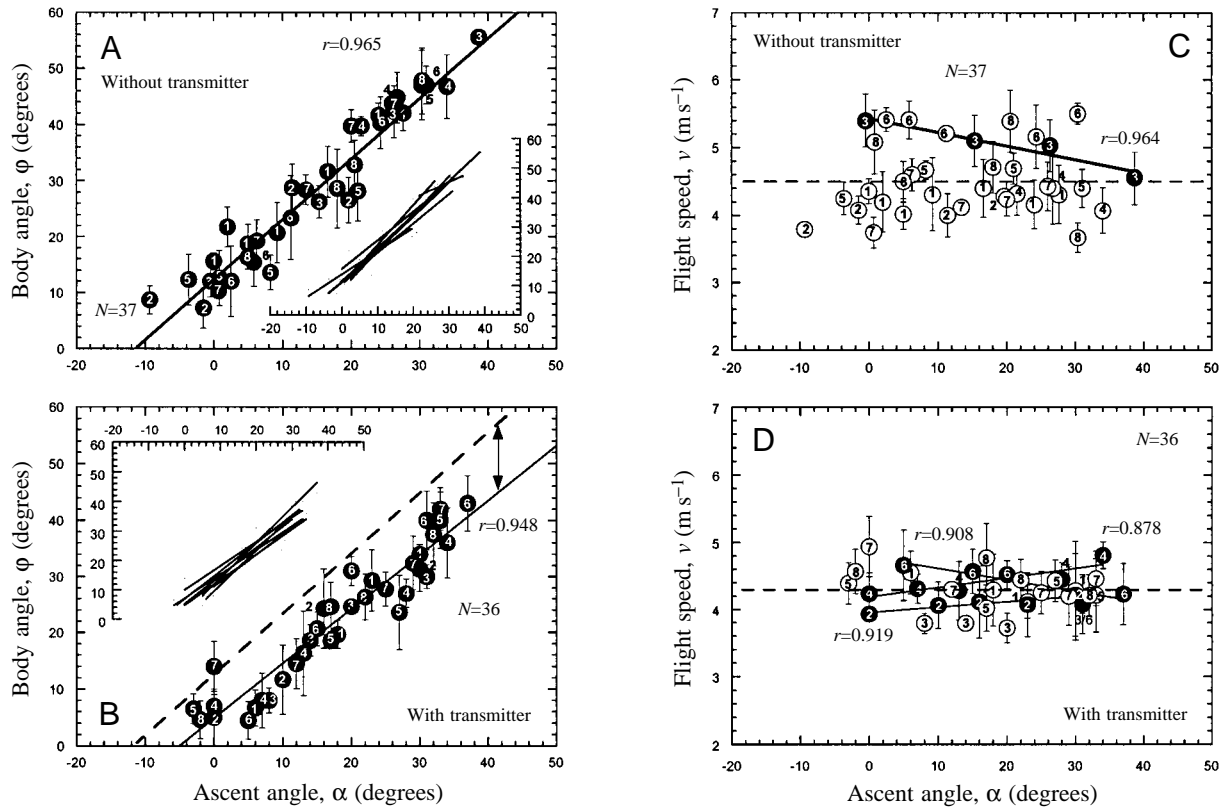


Fig. 2. Relationships between flight variables in eight adult female locusts *Schistocerca gregaria* during free flight. (A,B) Relationship between body angle ϕ and ascent angle α (A) under control conditions and (B) with a 0.3 g transmitter attached to the pronotum. Under both conditions, the body angle was significantly correlated with the ascent angle ($P < 0.05$, for equations, see Table 1). The insets in A and B show the regression lines obtained for the eight individuals investigated (all regressions were significant, $P < 0.05$). The numbers 1–8 within the filled circles indicate the individual. The dashed line in B is the relationship for control conditions (taken from A). $\Delta\phi$ indicates a systematic difference in body angle between the two experimental conditions. (C,D) Relationship between flight speed v and ascent angle α under control (C) and under loaded (D) conditions. Open circles represent data from individuals (numbered 1–8, same as in A,B) in which no significant correlation between v and α was observed. For control and loaded conditions, no significant correlation between flight speed and ascent angle was observed for the population ($P > 0.05$); however, one control (animal 3) significantly decreased its flight speed during climbing ($P < 0.05$; C). Under loaded conditions, two animals (animals 2, 4) increased and one animal (animal 6) decreased their flight speed (indicated by filled circles in C and D) during climbing. Data points represent mean \pm s.d. from 4–7 observations. For each individual, data from several flight sequences were pooled.

In each experimental animal, the body angle ϕ was significantly correlated with the ascent angle α for control flights and for flights with the transmitter attached (see insets of Fig. 2A,B, $P < 0.05$ in all individual regressions). The slopes of the two 'average' regressions did not differ significantly between the different conditions: ϕ increased by $1.087 \text{ degree degree}^{-1}$ of α when climbing in control flights ($r = 0.965$, $N = 37$, $P < 0.05$; Fig. 2A) and by $0.95 \text{ degree degree}^{-1}$ of α under transmitter load ($r = 0.948$, $N = 36$, $P < 0.05$; Fig. 2B; for equations, see Table 1). The range of instantaneous ascent angles observed during the flights under both conditions was comparable (loaded: -3 to 36° ; controls: -10 to 40°). However, a significant difference ($P < 0.05$) was found in the intercepts, indicating a systematic decrease in the body angle ($\Delta\phi$, Fig. 2B) when a transmitter was attached. This angle, deduced from the regressions the body angle, e.g. during level flight (i.e. $\alpha = 0^\circ$), was $\phi = 12.5^\circ$ in control animals, whereas the same animals exhibited a lower body angle ($\phi = 5.2^\circ$) during level flight under loaded conditions.

In seven females, flight speed was not significantly correlated with the ascent angle α during control flight ($P > 0.05$), but in one animal, the flight speed decreased significantly ($P < 0.05$) during climbing (Fig. 2C). For flight under loaded conditions, flight speed was not correlated with α in five females ($P > 0.05$, Fig. 2D), while two individuals exhibited a significant increase in speed when climbing, and one animal exhibited a significant decrease in flight speed during climbing ($P < 0.05$). The mean flight speed for the population under control conditions was $4.48 \pm 0.49 \text{ m s}^{-1}$ (mean \pm s.d., $N = 37$); when flying with the transmitter, the mean flight speed v was slightly but significantly lower ($v = 4.28 \pm 0.28 \text{ m s}^{-1}$, $N = 36$, $P < 0.05$). However, only in two of the eight individuals was a strong decrease in flight speed observed when loaded with a transmitter (animals 3 and 6, $P < 0.05$; see Fig. 2C,D).

These findings indicate that the attachment of a 0.3 g transmitter systematically influenced the values of particular flight variables such as the body angle; however, the findings

Table 1. Free-flight variables as a function of the ascent angle α in adult female locusts *S. gregaria* at 34 °C

Variable	Linear correlation coefficient, r	N
Body angle, ϕ		
$\phi(\alpha)_{\text{control}} = 12.54 + 1.087\alpha$	0.965	37
$\phi(\alpha)_{\text{transmitter}} = 5.19 + 0.955\alpha$	0.948	36
Stroke amplitude, Ψ		
$\Psi_{\text{hw}}(\alpha) = 103.39 + 0.453\alpha$	0.510	32
$\Psi_{\text{fw}}(\alpha) = 104.26 + 0.585\alpha$	0.618	32
Onset of wing elevation, ϕ_{el}		
$\phi_{\text{el}}^{\text{hw}}(\alpha) = 0.5507 + 0.959 \times 10^{-3}\alpha$	0.473	32
$\phi_{\text{el}}^{\text{fw}}(\alpha) = 0.5504 + 0.999 \times 10^{-3}\alpha$	0.512	32
Phase values $\phi_{\text{D/E}}$ of the hindwing antagonists examined		
$\phi_{179/119}(\alpha) = 0.5550 + 0.00157\alpha$	0.574	64
$\phi_{129/113}(\alpha) = 0.6160 + 0.00076\alpha$	0.401	53
$\phi_{127/113}(\alpha) = 0.5523 + 0.00239\alpha$	0.655	60
Phase values $\phi_{\text{E-D}}$ of the forewing antagonists examined		
$\phi_{99/90}(\alpha) = 0.5201 + 0.00102\alpha$	0.289	56
$\phi_{99/83}(\alpha) = 0.5537 + 0.00228\alpha$	0.582	56
$\phi_{97/83}(\alpha) = 0.4973 + 0.00169\alpha$	0.521	53

fw, forewing; hw, hindwing; $\phi_{\text{D/E}}$, phase value of elevator (E) activation within the depressor (D) cycle; 83, 90, 97, 99, 113, 119, 127, 129, muscle names according to Snodgrass (1929).

do not provide sufficient evidence to support the assumption that the functional relationships between the flight variables investigated here were changed substantially.

In 12 females (18 days postmoult, without a transmitter), the instantaneous wingbeat frequencies f_{WB} were determined by high-speed video and were related to the ascent angle. Each female performed 20 flights (including flights that were out of the camera focus). The results are shown in Fig. 3. In nine of the 12 locusts (i.e. in 75% of the animals investigated), no significant correlation between f_{WB} and ascent angle was observed ($P > 0.05$). A significant increase in f_{WB} during climbing was found in the remaining three animals (animals 5, 8 and 10 in Fig. 3, $P < 0.05$). The mean value of f_{WB} for all animals investigated at 34 °C was 24.4 ± 1.07 Hz ($N = 44$, mean \pm S.D.).

Wingstroke variables during climbing flight

In eight young adult females, the stroke amplitude Ψ and the phase of wing elevation within the downstroke cycle (ϕ_{el}) of the hindwing and the forewing were determined and plotted in relation to the ascent angle during climbing flight (Fig. 4). The animals used were younger (11–13 days postmoult) than the animals investigated in the previous sections; their mean wingbeat frequency f_{WB} was 23.2 ± 1.12 Hz ($N = 28$, mean \pm S.D.). The use of younger animals enhanced the numbers of frames per wingbeat cycle obtained using high-speed video recording (an average of 22 frames per cycle compared with

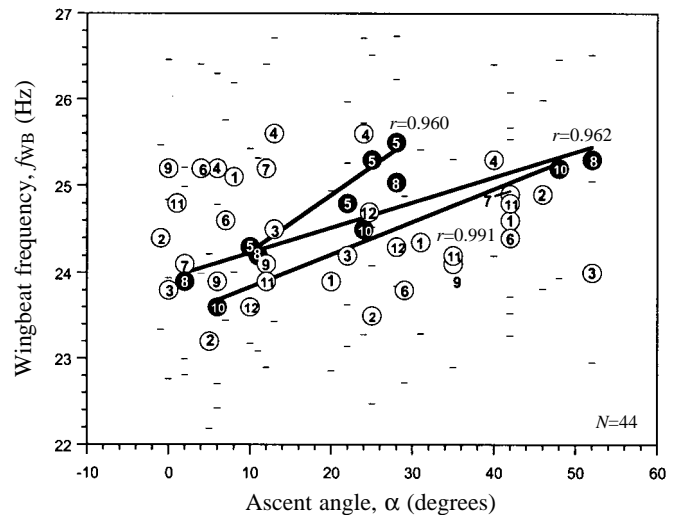


Fig. 3. Instantaneous wingbeat frequencies f_{WB} during flights with different ascent angles α in 12 adult female *Schistocerca gregaria* at 34 °C. Data points represent means \pm S.D. (small bars) from five consecutive wingbeat cycles. Data points are numbered 1–12, indicating the particular individual. Filled circles mark those individuals in which f_{WB} and α were significantly correlated ($P < 0.05$), and open circles are used when no correlation was observed ($P > 0.05$). In each individual, data from different flight sequences were pooled, individual regressions were based on $N = 4$ data points (except for animal 10, for which $N = 3$). The mean f_{WB} of the 12 animals was 24.4 ± 1.07 Hz ($N = 44$).

an average of 20 frames per cycle in adult mature females when recording at $500 \text{ frames s}^{-1}$). Individuals were evaluated only when data from both the hindwing and the forewing could be acquired.

In four of the eight females, the stroke amplitude of the forewing Ψ_{fw} increased significantly during climbing ($P < 0.05$, Fig. 4A). A significant increase in the stroke amplitude of the hindwing Ψ_{hw} was found in five of the eight animals ($P < 0.05$, Fig. 4B). However, in only two animals (animals 3 and 5, compare Fig. 4A,B) could an increase in both Ψ_{fw} and Ψ_{hw} be observed.

In four of the eight individuals, the phase of forewing elevation ϕ_{el} increased significantly in relation to the ascent angle ($P < 0.05$, Fig. 4C), and a significant increase in ϕ_{el} of the hindwing was found in four animals (Fig. 4D). An increase in ϕ_{el} in both the forewing and hindwing was observed in three of the eight individuals (animals 1, 2 and 3, see Fig. 4C,D).

The relationships between the wingstroke variables for all eight females are summarised in Table 2. The data for all individuals were pooled to obtain a mean slope and intercept for each wing; the regressions ($P < 0.05$; for equations, see Table 1) indicate (a) that the increase in stroke amplitude with increasing ascent angle α was more marked in the forewing than in the hindwing (the slopes are significantly different, $P < 0.05$, $N = 32$, but not the intercepts), and (b) that there was no difference in ϕ_{el} between the two wings (the slopes and intercepts are not significantly different in the hindwing and forewing, $P > 0.05$).

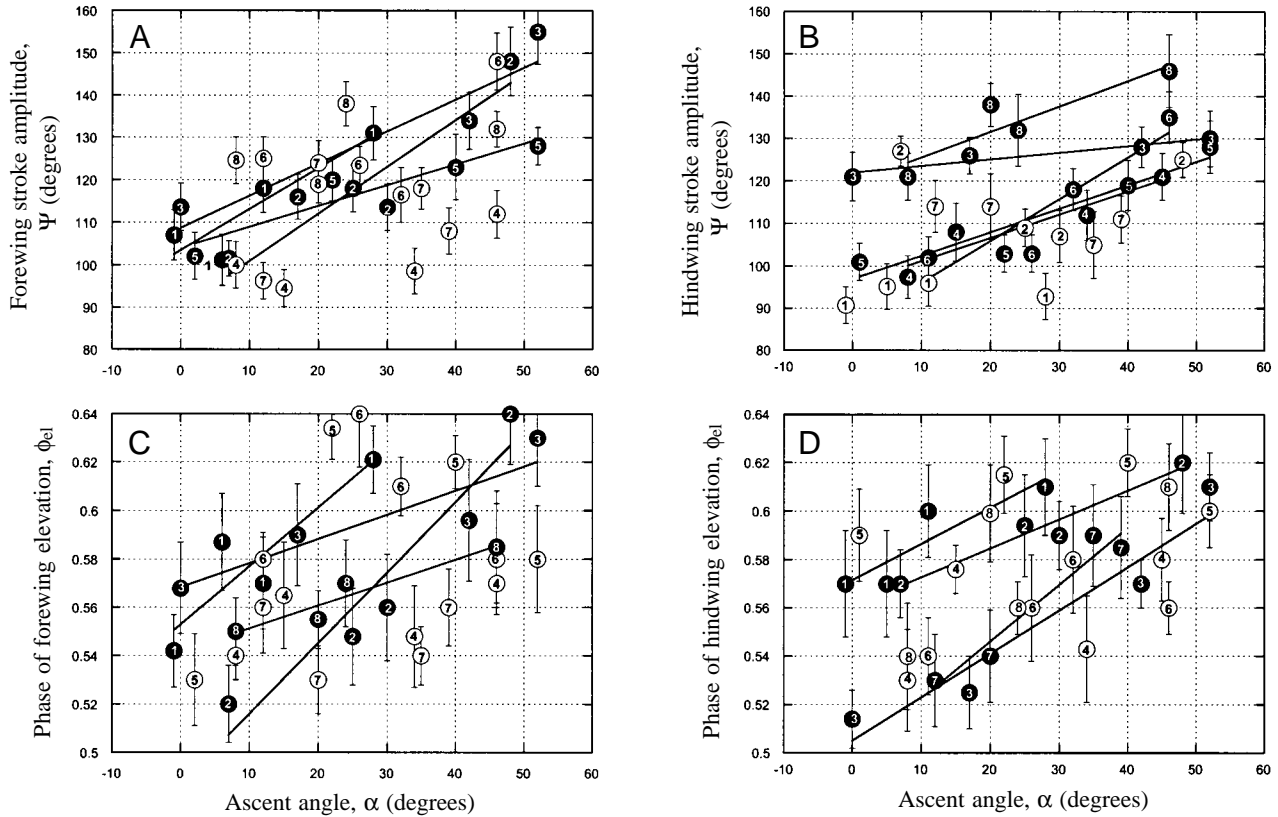


Fig. 4. Wingstroke variables during climbing free flight for eight young adult female *Schistocerca gregaria* (11–13 days postmoult) at 34 °C. For the hindwing and forewing, the stroke amplitudes Ψ (A,B) and the phases of wing elevation within the downstroke cycle ϕ_{el} (C,D) are plotted *versus* the ascent angle α . Filled circles indicate individuals (numbered 1–8) in which Ψ and ϕ_{el} were significantly correlated with α ($P < 0.05$, see Table 2), and open circles show individuals for which the correlation was not significant ($P > 0.05$). Data points represent means \pm s.d. from five consecutive wingbeat cycles. In each individual, data were pooled from different flight sequences.

The mean phase relationship between the hindwing and forewing (i.e. the interval between downstroke onset in the two wings) was 0.16 ± 0.03 (mean \pm angular deviation; $r = 0.956$, $N = 32$), with the hindwing leading. This phase relationship did not change significantly with increasing ascent angle α ($P > 0.05$, data not shown).

Table 2. Changes in stroke amplitude (Ψ) and phase of wing elevation (ϕ) of the hind- (hw) and the forewing (fw) with respect to the ascent angle α

Individual	Ψ_{hw}	ϕ_{hw}	Ψ_{fw}	ϕ_{fw}	N
1	NS	$r = 0.902$	$r = 0.905$	$r = 0.904$	4
2	NS	$r = 0.976$	$r = 0.946$	$r = 0.915$	4
3	$r = 0.999$	$r = 0.973$	$r = 0.942$	$r = 0.915$	4
4	$r = 0.948$	NS	NS	NS	4
5	$r = 0.994$	NS	$r = 0.948$	NS	4
6	$r = 0.917$	NS	NS	NS	4
7	NS	$r = 0.972$	NS	NS	4
8	$r = 0.956$	NS	NS	$r = 0.951$	4

r , coefficient of correlation ($P < 0.05$); NS, no significant correlation ($P > 0.05$).

Individuals correspond to the numbering shown in Fig. 4.

Flight motor patterns during free climbing flight

To measure changes in the motor pattern related to the ascent angle α during free climbing flight, telemetric recordings were made from several pairs of muscle antagonists in both wing segments. In different experimental sets, each pair of antagonists was investigated in 10 adult mature females (18–20 days postmoult) at a temperature of 34 °C. Each individual performed 10 flight sequences (including those not in the camera focus), and a further 10 flights were conducted after a 1 h break followed by warming-up.

For one individual, the antagonistic patterns of the first basalar depressor (127) and the tergosternal elevator (113, Fig. 5A) are shown in relation to the corresponding flight variables (Fig. 5B,C). During flight, this particular animal increased its ascent angle α continuously. The phase difference $\phi_{127/113}$ between the recorded activity of the depressor (127) and the elevator (113) increased with increasing values of α . This indicates that, in this flight sequence, the onset of elevator (113) activity was delayed with respect to the onset of depressor (127) activity when the animal performed climbing flight.

For both wings, the phase relationships between the antagonistic muscle pairs in relation to the ascent angle α are shown in Fig. 6. The relationships obtained for each of the 10

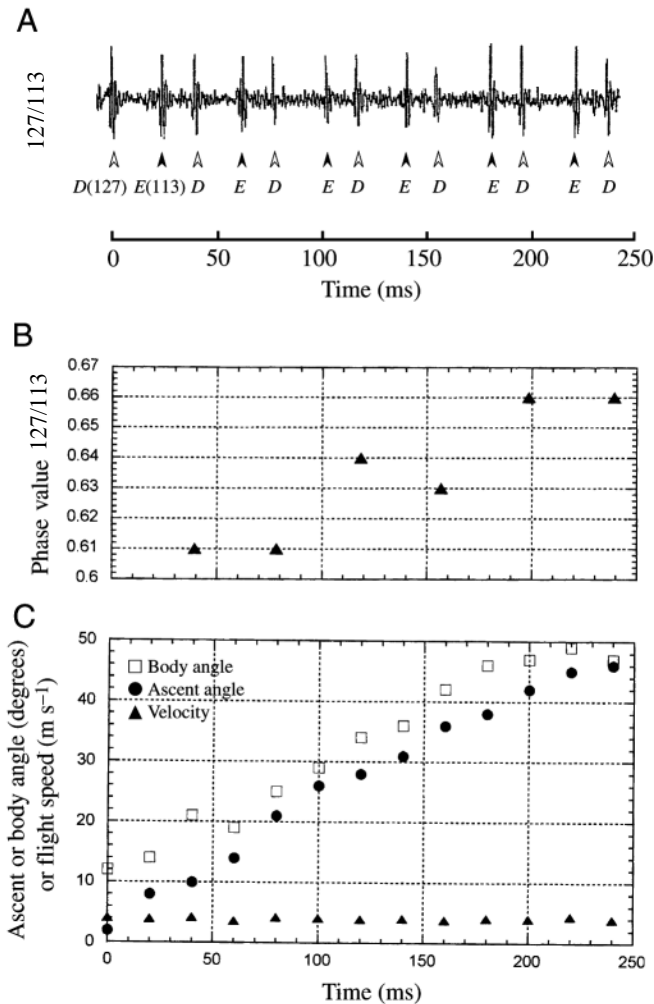


Fig. 5. Antagonistic motor pattern and corresponding flight variables of an individual that increased its ascent angle continuously during free flight. (A) Telemetric electromyogram trace of the first basalar depressor 127 (D) and the elevator 113 (E) of the hindwing. (B) Phase values of the elevator activity corresponding to A. (C) Ascent angle (●, degrees), body angle (□, degrees) and flight speed (▲, m s^{-1}) during the flight sequence. All variables are related to a common time scale (in ms). For details, see text.

animals tested in each experimental set are shown by insets in Fig. 6. To monitor the motor behaviour of the 'average' locust, the data for the 10 individuals tested were pooled to obtain a mean slope and intercept of the regression for each pair of antagonists (main parts in Fig. 6A,B; for equations, see Table 1).

For the antagonists of the hindwing, the phase values in relation to the ascent angle α are shown in Fig. 6A: the phase values of the hindwing elevators 119 (Fig. 6Ai) and 113 (Fig. 6Aii) increased significantly with increasing α ($P < 0.05$). This indicates that both elevator muscles were delayed in their onset with respect to the subalar 129 (depressor) cycle when the animals performed ascending flight. The phase relationship $\phi_{129/119}$ was in general lower than $\phi_{129/113}$ (the intercepts were significantly different, $P < 0.05$): this means that muscle 119 is

activated earlier during the wingbeat cycle than the synergist 113.

Comparable relationships were found for the forewing elevators 90 (Fig. 6Bi) and 83 (Fig. 6Bii) with respect to the subalar (99) depressor: both elevator synergists showed a significant delay in activation when the ascent angle was increased ($P < 0.05$). However, the shift in $\phi_{99/90}$ was weak compared with that in $\phi_{99/83}$ (slopes significantly different, $P < 0.05$, Table 1). The intercepts were significantly different ($P < 0.05$). This indicates that elevator 83 was activated later during the wingbeat cycle than elevator 90.

In addition, phase values of wing elevators (83, 113) were determined with respect to the first basalar depressors of each wing segment (97, 127). The results are shown in Fig. 6Aiii and Biii. In the hindwing, $\phi_{127/113}$ increased significantly ($P < 0.01$) with increasing α (Fig. 6Biii). The delay in 113 activation in relation to 127 activation was greater than with respect to 129 (slopes significantly different between $\phi_{127/113}$ and $\phi_{129/113}$, $P < 0.05$). This further indicates that the delay between the activation of the synergists 129 and 127 decreased with increasing ascent angle; both muscles are expected to be activated nearly synchronously at an ascent angle of approximately 40° (Fig. 6Aiii).

Considering the homonomous muscles in the forewing (elevator 83 and basalar 97), comparable results were obtained (Fig. 6Aiii, Biii): activity in 83 was delayed with respect to activity in 97 when the animals increased their ascent angle α . However, $\phi_{97/83}$ values were, in general, below those found for $\phi_{99/83}$ (intercepts significantly different, $P < 0.05$). This indicates that, with respect to 83, the first basalar (97) is activated later than the subalar (99) muscle within the wingbeat cycle. A scheme for the activation of the antagonists examined in these experiments with respect to climbing flight was deduced from Table 1 and is shown in Fig. 7.

Discussion

In the present study, the onset of elevator muscle activity during the wingbeat cycle was investigated telemetrically with respect to the ascent angle during free locust flight. In the majority of individuals tested, the wing elevator muscles examined were delayed in their activation with respect to the synchronously recorded wing depressor muscle. Corresponding to the alterations in motor pattern, an increase in the phase of wing elevation (i.e. delayed wing elevation) and/or an increase in the stroke amplitude was observed. These findings suggest that the relative timing of elevator activity during flight not only contributes to a functional motor pattern (e.g. Wolf, 1993) but also plays a functional role in regulating the ascent angle during climbing flight.

Flight variables and aerodynamics

The application of unsteady aerodynamic calculations to the flapping flight of insects such as locusts has enabled a basic understanding of the relationships between wing kinematic variables and the aerodynamic forces produced by the wing

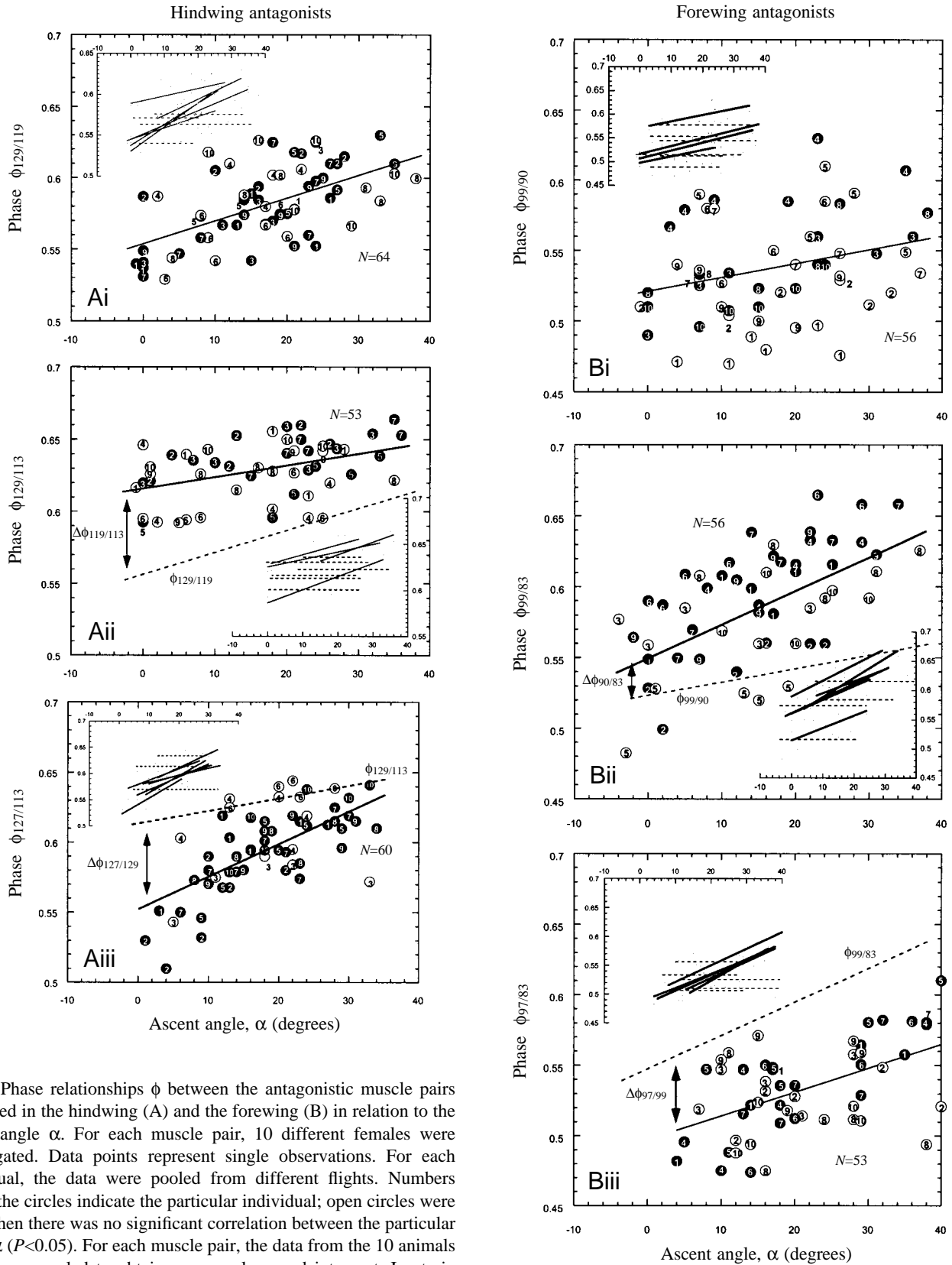


Fig. 6. Phase relationships ϕ between the antagonistic muscle pairs examined in the hindwing (A) and the forewing (B) in relation to the ascent angle α . For each muscle pair, 10 different females were investigated. Data points represent single observations. For each individual, the data were pooled from different flights. Numbers within the circles indicate the particular individual; open circles were used when there was no significant correlation between the particular ϕ and α ($P < 0.05$). For each muscle pair, the data from the 10 animals tested were pooled to obtain a mean slope and intercept. Insets in i–iii show the relationships for each individual; solid lines indicate a significant correlation between the variables ($P < 0.05$), and dashed lines are used in those individuals in which no significant correlation was found ($P > 0.05$). For comparison, dashed lines in the main parts

Aii,iii and Bii,iii show the relationships found for the other antagonists examined within the particular hemisegment. The phase relationships between synergists and their changes in relation to α are indicated by $\Delta\phi$.

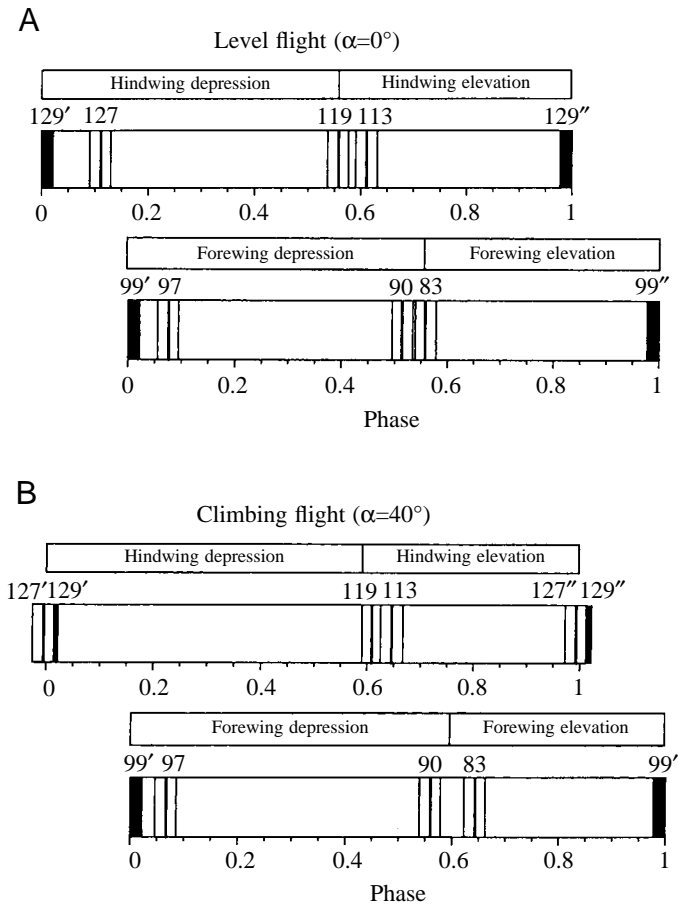


Fig. 7. Scheme of the activation of hindwing and forewing antagonists during the wingbeat cycle during level flight (A) and during steep climbing flight (B) of the 'average' locust. Phase values were deduced from Table 1, and bar width represents the 5% confidence interval. The hindwing constantly leads the forewing (see text). For both the hindwing and the forewing, the phase values between the muscle antagonists increase when the animal increases its ascent angle (compare $\alpha=0^\circ$ in A with $\alpha=40^\circ$ in B). In both the hindwing and forewing, these delays in elevator muscle activation correspond to a delay in the elevation of the particular wing when the animal performs climbing flight. Except for 90/83, the delay in activation between the synergist muscle pairs (129/127, 99/97, 119/113 and 90/83) decreases with increasing α .

movement (Send, 1992, 1994; Zarnack and Send, 1994; Zarnack, 1997). In locust flight, the main implications of this theory are as follows. (1) The functional task of the complex wing movements, i.e. alternating up and down movement, cyclic changes in the wing angle of attack, and wing pro- and remotion along the longitudinal body axis ('lagging'), is the generation of thrust not lift. (2) The generation of lift during the wing beat relies on the steady wing angle of attack and on the speed of the air stream faced by the wing profile, i.e. the flight speed. However, (3) wingstroke amplitude and wingbeat frequency have only weaker influences on lift production. Applying the theory of unsteady aerodynamics, some functional implications can be deduced for a transition from level to climbing flight: in general, climbing requires additional

lift production, i.e. the output of additional effective lifting power (e.g. Fischer and Ebert, 1999). Since lift generation depends mainly on the steady wing angle of attack during flight, additional lift can be generated by increasing the air speed faced by the wing profile. Theoretically, this can be achieved by increasing flight speed.

Our findings during free flight show that no significant correlation between f_{WB} and the ascent angle was present in the majority of animals (Fig. 3; see also Baker et al., 1981). This means that the generation of additional lift during climbing is, apparently, not achieved by increasing the wingbeat frequency (see topic 3 above). Approximately half the animals tested during free flight increased the stroke amplitude of the hindwing or the forewing during climbing (Fig. 4). In the majority of the animals investigated, flight speed was not correlated with the ascent angle (Fig. 2).

Since increasing the stroke amplitude causes a small but significant increase in lift during tethered flight (Wortmann and Zarnack, 1993), we conclude that the additional lift required for climbing flight is generated, at least partly, by an increase in the stroke amplitude of a particular wing.

As shown in Table 2, a delay in wing elevation with respect to the ascent angle was also observed in animals that did not synchronously increase the stroke amplitude of that particular wing (although stroke amplitude and phase of elevation in at least one of the wings were positively correlated in three of eight animals investigated). The most likely explanation is that stroke amplitude and the phase of wing elevation during the wingbeat cycle may have different tasks and, thus, may rely on different control mechanisms during flight. It is unclear whether elongating the duration of the downstroke by shifting the phase of wing elevation results in an increase in flight speed.

Body angle and ascent angle are strongly correlated, suggesting a significant role for the body angle in the production of additional lift (Fig. 2; see also Baker et al., 1981). This is confirmed by reports showing that adjusting the locust body angle reproducibly manipulates lift generation (Wortmann and Zarnack, 1993). However, it is not clear which variables control the body angle during free flight.

In our study, the phase value between the two wings did not change with changing ascent angle. As reported previously, relative lift production depends on an appropriate delay between the two flapping wing pairs (maximum lift is generated at $\Delta t=8$ ms in tethered flying locusts; Wortmann and Zarnack, 1993). This indicates that the additional lift production required for climbing flight is not, apparently, generated by a phase shift between the hind- and the forewing, since changes in this phase value are expected to reduce lift production in general.

The timing of wing elevation during climbing flight

Appropriate timing of the elevator muscles during the wingbeat cycle seems to be an important functional task during flight pattern generation. This becomes evident from the fact that, in particular, elevator activation can be influenced by proprioceptive input (e.g. by signals from tegula organs and

wing hinge stretch receptors; Wolf and Pearson, 1988; Pearson and Wolf, 1989) and that the timing of elevator activity onset is affected after sensory deafferentation (Büschges and Pearson, 1991; Büschges et al., 1992; Wolf, 1993). The timing of elevator activity determines the stroke amplitude of the wing (e.g. Hedwig and Becher, 1998). Our suggestion that the timing of elevator activity plays a functional role in regulating the ascent angle during climbing flight is further supported by recent findings during free locust flight. Although the general capability for free flight is maintained, ablation of the tegula organs not only affects the elevator timing (Fischer and Ebert, 1999) but is also responsible for impaired flight behaviour (Gee and Robertson, 1998): the power output of the flight system was reduced, and the range of ascent angles observed after tegula removal was significantly decreased (Fischer and Ebert, 1999).

Free-flight motor patterns during climbing flight

The functional role of activating a particular wing muscle in the complex three-dimensional wing movement is difficult to evaluate. Together with flight muscles that were not recorded in our study, the relative activity of the antagonists investigated is reported not only to determine the downstroke interval and, hence, the phase of wing elevation and stroke amplitude (e.g. Hedwig and Becher, 1998), but also to control the wing angle of attack (Wilson and Weis-Fogh, 1962; Pfau, 1977, 1978, 1982) that is co-responsible for thrust production (for an overview, see Zarnack, 1997). The motor pattern recorded during free flight therefore represents a 'superimposed image' with respect to at least two functional tasks (i.e. climbing, see this paper) and the control of lateral stability (Möhl, 1985). Alterations in the pattern due to steering and corrective steering (e.g. Robert, 1988) cannot be excluded completely; however, our study focused on straight forward flights, and flights with any visible sign of directional changes within the horizontal plane were excluded from evaluation.

In this study, the activity onsets of the first (113, 83) and second (119, 90) tergosternal elevator muscles were examined with respect to the onsets of the subalar (129, 99) and first basalar (127, 97) depressor muscles in the meso- and metathoracic segments. Our findings indicate that ascent-dependent phase changes are different for the particular antagonistic muscles investigated (Figs 6, 7). In many previous studies, locust flight motor patterns have been monitored by recording from a single pair of antagonists (127/113, e.g. Büschges and Pearson, 1991; 97/83, e.g. Wolf, 1993; 129/119 and 90/99, e.g. Stevenson and Kutsch, 1987). When focusing on only one pair of antagonists, general conclusions, for example how strongly sensory input modulates motor pattern generation (Wolf and Pearson, 1987; Stevenson and Kutsch, 1987), might be misleading (i) because, during the wingbeat cycle, the timing of the muscles investigated differs, in general, from that of other hemisegmental synergists, and (ii) because the timing of a particular muscle may be influenced strongly by proprioceptive input, whereas the timing other synergists,

although in the same wing segment, may be only weakly influenced (Möhl, 1993).

Given the present state of knowledge, we cannot conclude from our free-flight investigation that there is an altered 'basic' mechanism of flight pattern generation during tethered flight since (i) the basic relationships between the free-flight variables match the findings and their aerodynamic implications found in tethered studies (e.g. Zarnack and Wortmann, 1989; Wortmann and Zarnack, 1993; Zarnack, 1997) and (ii) the motor pattern is, in general, comparable with previous reports in tethered flight (e.g. Wolf and Pearson, 1987; Stevenson and Kutsch, 1987; Pearson and Wolf, 1989; Büschges and Pearson, 1991; Hedwig and Becher, 1998).

Free-flight variables in locusts: comparison between field and laboratory studies

In contrast to the well-documented behaviour of migrating locust swarms with respect to environmental variables in the southern hemisphere (for a review, see Farrow, 1990), there is little field information about individual flyers (Waloff, 1972; Baker and Cooter, 1979a,b; Baker et al., 1981). The relationships between body angle, wingbeat frequency, flight speed and ascent angle match the findings of previous field observations. This is of particular interest (i) because the field observations were performed on *L. migratoria* (e.g. Baker et al., 1981) compared with our study of *S. gregaria*, and (ii) because the locusts observed in the field had become airborne at least 30 min before the data were acquired (Baker et al., 1981), whereas the majority of the animals investigated in our study had been flying for only a few seconds before data acquisition. This suggests that the relationships between free-flight variables investigated in both types of study are (i) comparable for both genders of both locust species and (ii) independent of the duration of flight (migrating 'long-term' flight or 'short-time' flights of approximately 30 s).

We are grateful to A. Büschges (Universität Köln) for a critical reading of the manuscript and to G. Wendler (Universität Köln) for valuable discussion. We wish to thank an anonymous referee for his constructive criticism and valuable suggestions. We thank especially C. Graef (Universität Köln) for her assistance. This project was supported by the DFG (Ku 240/17-1,2).

References

- Baker, P. S.** (1979a). The wing movements of flying locusts during steering behaviour. *J. Comp. Physiol. A* **131**, 49–58.
- Baker, P. S.** (1979b). The role of forewing muscles in the control of direction in flying locusts. *J. Comp. Physiol. A* **131**, 59–66.
- Baker, P. S. and Cooter, R. J.** (1979a). The natural flight of the migratory locust, *Locusta migratoria*. I. Wing movements. *J. Comp. Physiol. A* **131**, 79–87.
- Baker, P. S. and Cooter, R. J.** (1979b). The natural flight of the migratory locust, *Locusta migratoria*. II. Gliding. *J. Comp. Physiol. A* **131**, 89–94.

- Baker, P. S., Gewecke, M. and Cooter, R. J.** (1981). The natural flight of the migratory locust, *Locusta migratoria*. III. Wingbeat frequency, flight speed and attitude. *J. Comp. Physiol. A* **141**, 233–237.
- Batschelet, E.** (1981). *Circular Statistics in Biology*. London, New York: Academic Press.
- Büschges, A. and Pearson, K. G.** (1991). Adaptive modifications in the flight system of the locust after the removal of wing proprioceptors. *J. Exp. Biol.* **157**, 313–333.
- Büschges, A., Ramirez, J.-M. and Pearson, K. G.** (1992). Reorganization of sensory regulation of locust flight after partial deafferentation. *J. Neurobiol.* **23**, 31–42.
- Delcomyn, F.** (1980). Natural basis of rhythmic behaviour in animals. *Science* **210**, 492–498.
- Farrow, R. A.** (1990). Flight and migration in acroids. In *Biology of Grasshoppers* (ed. R. F. Chapman and A. Joern), pp. 227–313. New York: Wiley & Sons Inc.
- Fischer, H.** (1998). *Untersuchungen zur Verhaltensphysiologie freifliegender Heuschrecken unter Einsatz von Telemetrie*, vol. 347. Allensbach: UFO Atelier und Verlag GmbH.
- Fischer, H. and Ebert, E.** (1999). Tegula function during free locust flight in relation to motor pattern, flight speed and aerodynamic output. *J. Exp. Biol.* **202**, 711–721.
- Gee, C. E. and Robertson, R. M.** (1998). Free flight ability of locusts recovering from partial deafferentation. *Naturwissenschaften* **85**, 167–170.
- Gewecke, M.** (1975). The influence of air current sense organs on the flight behaviour of *Locusta migratoria*. *J. Comp. Physiol. A* **103**, 79–95.
- Hedwig, B. and Becher, G.** (1998). Forewing movements and intracellular motoneuron stimulation in tethered flying locusts. *J. Exp. Biol.* **201**, 731–744.
- Horsmann, U. and Wendler, G.** (1985). The role of a fast wing reflex in locust flight. In *Insect Locomotion* (ed. M. Gewecke and G. Wendler), pp. 153–165. Berlin, Hamburg: Paul Parey.
- Kutsch, W., van der Wall, M. and Fischer, H.** (1999). Analysis of free forward flight of *Schistocerca gregaria* employing telemetric transmission of muscle potentials. *J. Exp. Zool.* **284**, 119–129.
- Möhl, B.** (1985). The role of proprioception in locust flight control. I. Asymmetry and coupling within the time pattern of motor units. *J. Comp. Physiol. A* **156**, 93–101.
- Möhl, B.** (1993). The role of proprioception for motor learning in locust flight. *J. Comp. Physiol. A* **172**, 325–332.
- Neumann, L., Möhl, B. and Nachtigall, W.** (1983). Untersuchungen zur Funktion der Tegula bei fliegenden Heuschrecken (*Locusta migratoria* L.). In *Biona Report 2* (ed. W. Nachtigall), pp. 89–104. Stuttgart, New York: Gustav Fischer.
- Pearson, K. G. and Wolf, H.** (1987). Comparison of motor patterns in the intact and deafferented flight system of the locust. I. Electromyographic analysis. *J. Comp. Physiol. A* **160**, 259–268.
- Pearson, K. G. and Wolf, H.** (1989). Timing of forewing elevator activity during flight in the locust. *J. Comp. Physiol. A* **165**, 217–227.
- Pfau, H. K.** (1977). Zur Morphologie und Funktion des Vorderflügels und Vorderflügelgelenks von *Locusta migratoria* L. *Fortschr. Zool.* **24**, 341–345.
- Pfau, H. K.** (1978). Funktionsanatomische Aspekte des Insektenfluges. *Zool. Jb. Anat.* **99**, 99–108.
- Pfau, H. K.** (1982). Mechanik und sensorische Kontrolle der Flügel – Pronation und Supination. In *Biona Report 1* (ed. W. Nachtigall), pp. 61–77. Stuttgart New York: Gustav Fischer.
- Ramirez, J.-M. and Pearson, K. G.** (1993). Alteration of bursting properties in interneurons during locust flight. *J. Neurophysiol.* **70**, 2148–2160.
- Reye, D. N. and Pearson, K. G.** (1988). Entrainment of the locust central flight oscillator by wing stretch receptor stimulation. *J. Comp. Physiol. A* **162**, 77–89.
- Robert, D.** (1988). Visual steering under closed-loop conditions by flying locusts: flexibility of the optomotor response and mechanisms of correctional steering. *J. Comp. Physiol. A* **164**, 15–24.
- Robertson, M. and Pearson, K. G.** (1985). Neural circuits in the flight system of the locust. *J. Neurophysiol.* **53**, 110–128.
- Sachs, L.** (1978). *Angewandte Statistik*, fifth edition. Berlin: Axel Springer.
- Schmidt, J. and Zarnack, W.** (1987). The motor pattern of locusts during visually induced rolling in long-term flight. *Biol. Cybernetics* **56**, 397–410.
- Send, W.** (1992). The mean power of forces and moments in unsteady aerodynamics. *Z. Angew. Math. Mech.* **72**, 113–132.
- Send, W.** (1994). Basic description of animal flight. *Proceedings of the 22nd Goettingen Neurobiology Conference*, vol. II (ed. N. Elsmer and H. Breer), p. 273. Stuttgart, New York: Georg Thieme.
- Snodgrass, R. E.** (1929). The thoracic mechanisms of a grasshopper and its antecedents. *Smith. Misc. Collns* **82**, 1–111.
- Stevenson, P. A. and Kutsch, W.** (1987). A reconsideration of the central pattern concept for locust flight. *J. Comp. Physiol. A* **161**, 115–129.
- Thüring, D. A.** (1986). Variability of motor output during flight steering in locusts. *J. Comp. Physiol. A* **158**, 653–664.
- van der Wall, M.** (1996). Muskelaktivität während des Freifluges von Heuschrecken (Ein-Kanal-Telemetrie). Diploma thesis, University of Konstanz.
- Waloff, Z.** (1972). Observation on the airspeed of freely flying locusts. *Anim. Behav.* **20**, 367–372.
- Weis-Fogh, T.** (1956). Biology and physics of locust flight. II. Flight performance of the desert locust (*Schistocerca gregaria*). *Phil. Trans. R. Soc. Lond. B* **239**, 459–510.
- Wendler, G.** (1974). The influence of proprioceptive feedback on locust flight co-ordination. *J. Comp. Physiol. A* **88**, 173–200.
- Wilson, D. M. and Weis-Fogh, T.** (1962). Patterned activity of co-ordinated motor units, studied in flying locusts. *J. Exp. Biol.* **39**, 643–667.
- Wolf, H.** (1993). The locust tegula: significance for flight rhythm generation, wing movement control and aerodynamic force production. *J. Exp. Biol.* **182**, 299–253.
- Wolf, H. and Pearson, K. G.** (1987). Comparison of motor patterns in the intact and deafferented flight system of the locust. II. Intracellular recordings of the flight motoneurons. *J. Comp. Physiol. A* **160**, 269–279.
- Wolf, H. and Pearson, K. G.** (1988). Proprioceptive input patterns elevator activity in the locust flight system. *J. Neurophysiol.* **59**, 1831–1853.
- Wortmann, M. and Zarnack, W.** (1993). Wing movements and lift regulation in the flight of desert locusts. *J. Exp. Biol.* **182**, 57–69.
- Zarnack, W.** (1997). Kinematik und Aerodynamik des Heuschreckenfluges. In *Biona Report II* (ed. W. Nachtigall), pp. 173–200. Stuttgart, Jena, Lübeck, Ulm: Gustav Fischer.
- Zarnack, W. and Möhl, B.** (1977). The activity of the direct downstroke muscles of *Locusta migratoria* (L.) during steering

behaviour in flight. I. Patterns of time shift. *J. Comp. Physiol. A* **118**, 235–247.

Zarnack, W. and Send, W. (1994). Applications of unsteady aerodynamics to the locust flight. *Proceedings of the 22nd*

Goettingen Neurobiology Conference, vol. II (ed. N. Elsmer and H. Breer), p. 274. Stuttgart, New York: Georg Thieme.

Zarnack, W. and Wortmann, M. (1989). On the so-called constant lift reaction of migratory locusts. *J. Exp. Biol.* **147**, 111–123.